Measurement 208 (2023) 112461

Contents lists available at ScienceDirect

Measurement

journal homepage: www.elsevier.com/locate/measurement

Investigation of the performance of mock-target IR thermography for indoor air temperature measurements under transient conditions

Loucas Georgiou [a], .Laura Stasiuliene [b], Rokas Valancius [b], Lina Seduikyte [b], Andrius Jurelionis [b], Paris A. Fokaides [a,b,*]

[a] Frederick University, School of Engineering, Cyprus
[b] Kaunas University of Technology, Faculty of Civil Engineering and Architecture, Lithuania

ARTICLE INFO

Keywords:
IR thermography
Indoor air temperature
Environmental chamber
Finite element method
Mock target
Transient conditions

ABSTRACT

Mock Target IR Thermography for indoor air temperature measurement has been proven as an effective methodology for steady-state conditions. This method uses vertical poles of known emissivity placed in a space to measure air temperature by employing IR thermography. Compared to thermocouple / point-by-point measurement, this technique allows obtaining air temperature values in a continuous line. Several poles can be installed in a space ensuring the collection of a large amount of air temperature data entries by taking a single IR image, whereas measurements in large spaces with hundreds of thermocouples would require complicated wiring and data collection hardware. However, for this approach to be more widely considered, such measurement techniques should be adaptable for transient conditions as well, as air temperature can fluctuate and change due to external climatic conditions, occupancy or faults in HVAC equipment. This work aims to investigate if IR Thermography which was only tested in steady-state conditions can be applied to conditions of transient variation of indoor air temperature. For this purpose, measurements under lab conditions and numerical analysis with the use of finite element modelling (FEM) were performed. Specifically, measurements were carried out by using both Mock Target IR thermography and thermocouples, to investigate the precision of IR-obtained transient data. The experiments were conducted in the environmental chamber under controlled conditions. Three types of heating systems (underfloor heating, radiator heating, and ventilation heating) were investigated to ensure that the method is tested under conditions of different heat-emitting devices, as well as different convection and radiation ratios. Validated numerical models were developed using the FEM Multiphysics approach, to extend the scope of the assessment under various conditions and to observe the difference between the mock target pole temperature and air temperature. It was concluded that the mock target IR Thermography performance was accurate for the case of transient air temperature, as well as for different rates of temperature change, with an average temperature deviation of 0.4 [%] according to the experimental measurements and 1.74 [%] based on the numerical simulations.

1. Introduction

The use of IR thermography has proven to be a very useful method for the definition of the surface temperature of objects [13]. The technique exploits the principles of thermal radiation, as it quantifies the radiation emitted by a target, converting this information to a surface temperature [10]. The concept of the methodology is visualized in Fig. 1. The applicability of the method has been proven on many occasions in the scientific literature for the definition of the thermal conditions of complex geometries on a real-time basis [5]. Several studies have also combined IR thermography measurements with numerical simulation towards delivering thermal information related to objects [2]. The employment of thermography was further extended in recent years to active applications [17].

Recently applications of IR thermography for the definition of the performance of a building's ventilation and indoor conditions have been documented [21]. Particularly, the technique of measuring the indoor temperature using mock targets and IR thermography has proven in the recent past to be a very precise methodology with great prospects [9].

* Corresponding author at: Frederick University, School of Engineering, Cyprus.
E-mail addresses: res.gl@frederick.ac.cy (L. Georgiou), laura.stasiuliene@ktu.lt (.Laura Stasiuliene), rokas.valancius@ktu.lt (R. Valancius), lina.seduikyte@ktu.lt (L. Seduikyte), andrius.jurelionis@ktu.lt (A. Jurelionis), eng.fp@frederick.ac.cy, paris.fokaides@ktu.lt (P.A. Fokaides).

https://doi.org/10.1016/j.measurement.2023.112461
Received 2 July 2022; Received in revised form 17 December 2022; Accepted 8 January 2023
Available online 10 January 2023

Nomenclature

Symbol	Description Units
Cp	Specific heat capacity at constant stress [J/(kg·K)]
ΔQ_{ir}	Product of the temperature difference between the air and the sky and the external radiative heat transfer coefficient [W/m^2]
I	Global solar irradiance [W/m^2]
k	Thermal conductivity [W/mK]
N	Number of observations [-]
Q	Contains additional heat sources [W/m^3]
p	Pressure [Pa]
q	Heat flux by conduction [W/m^2]
s	Sample standard deviation [-]
S	Strain-rate tensor [1/s]
T	Absolute temperature [K]
v	Fluid Velocity [m/s]
Greek Symbol	Description Units
ρ	Density [kg/m^3]
τ	Viscous stress tensor [Pa]
Abbreviation	Description
FEM	Finite Element Method
IR	Infrared
HVAC	Heating, Ventilation and Air Conditioning

on the thermal comfort of occupants was investigated to distinguish the comfort levels considering environmental variable conditions. The main outcome of the studies was that the air temperature stratification resulted in thermal sensations differences caused by various non-uniform thermal environments [22,1,14].

In the study of Fokaides et al. [9] the mock target IR thermography technique was developed and introduced. This technique allows the measurement of the air temperature in indoor spaces. The method involves the use of mock targets with the appropriate geometry and thermal properties, to achieve thermal equilibrium with the air temperature in a short time. A similar approach was also documented in the study of Seiwert et al concerning the detection of vertical air temperature distribution by long-wave infrared thermography [19]. In this study, the functionality of a method for the measurement of stratification through the surface temperature of a single wall at steady-state conditions was demonstrated.

Although the first evidence in the scientific literature on this topic was positive concerning the appropriateness of the method for the definition of stratification characteristics, the method of mock target IR thermography was still not applied for transient conditions.

The purpose of this study is to investigate the applicability of this method under transient conditions, an innovative approach that reflects the real-world scenario compared to other studies where steady-transient boundary conditions have been applied. The structure of this report consists of the description of the materials and methods employed for the implementation of experimental and numerical investigation of the subject under discussion. The findings are discussed in detail in the third section of the study, and the main conclusions are given in the last section of this work. This study aspires to lay the path for the wider adoption of this method for measuring indoor thermal conditions with the use of a non-intrusive technique, in addition, to allow for data gathering which potentially can be used as boundary input for numerical model analysis.

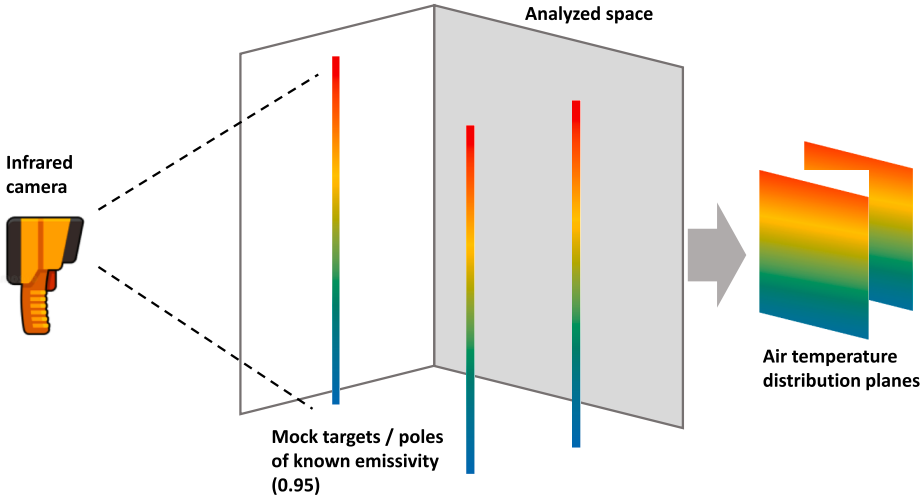

Fig. 1. Conceptual representation of the proposed method.

This measurement technique can be used for several problems, especially those related to the study of phenomena observed during indoor ventilation and air conditioning, such as the effect of stratification [8]. In the study of [4] experimental measurements and numerical investigations were performed revealing that the HVAC loads were affected by the thermal stratification and non-uniform thermal environments. In addition, energy consumption was investigated in the study of [16] and findings revealed that increasing the airflow supply directly increases energy consumption. Consequently improving thermal stratification and finding the optimal balance between air mixing effectiveness and energy efficiency can potentially reduce energy consumption. The importance of studying air distribution in spaces is also increasing for epidemiological reasons [18], the use of non-invasive methods, which can quickly and reliably provide information concerning HVAC systems operation and air temperature in space, is considered essential. In certain studies, the impact of air temperature stratification

2. Materials and methods

2.1. Test facility and equipment

In this study, the full-scale indoor environmental chamber at the Energy and Microclimate laboratory of the Kaunas University of Technology in Lithuania was employed (Fig. 2). The floor area of the chamber is 13 [m^2], and its volume is 35.8 [m^3]. This study focuses on the three most widely used heating emission systems of underfloor

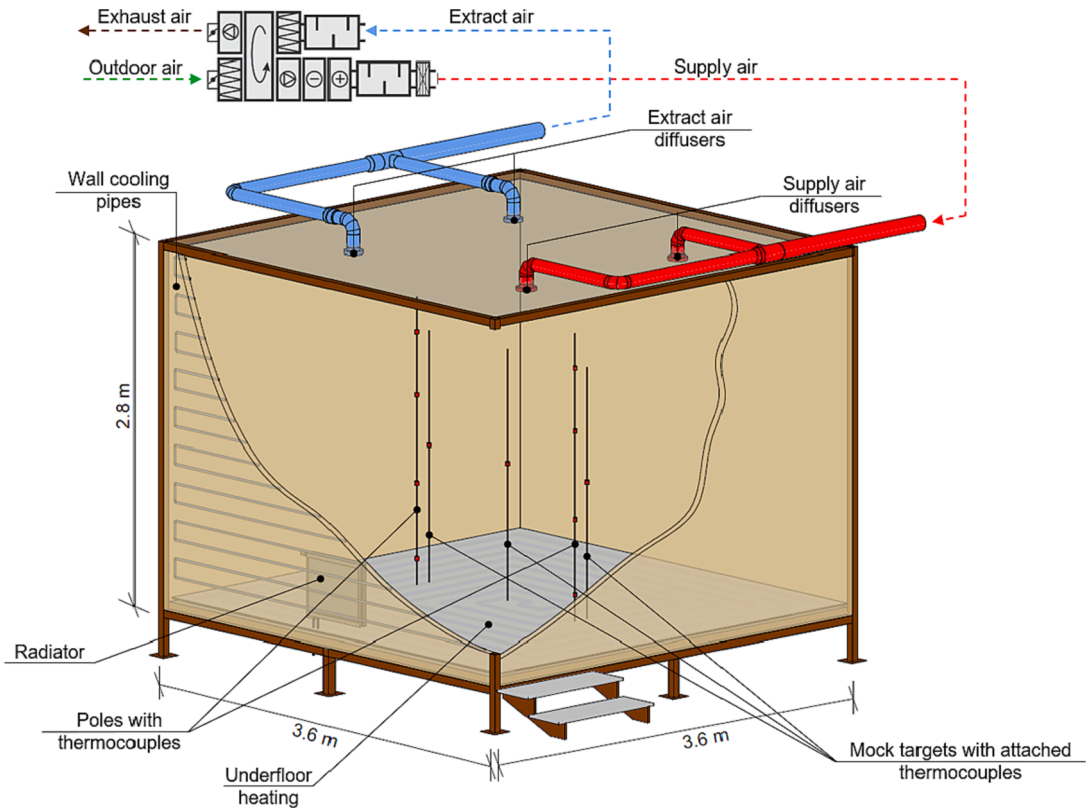

Fig. 2. Indoor environmental chamber at the Energy and Microclimate laboratory of, Kaunas University of Technology (Lithuania).

heating, radiator heating and air ventilation heating [15,6]. Considering the difference in the heat transfer pattern of convection and radiation [20,12] the investigation included both heat transfer mechanisms to provide a comprehensive investigation of the effectiveness of IR mock target thermography under different heat transfer conditions. Air supply and extraction conditions are controlled by an air handling unit (GOLD 04, Swegon AB, Sweden) in combination with a water-borne air heater and cooler. Concerning the radiator and underfloor heating, pre-heated water with the use of a (Ray, Protherm, Czech Republic) electric boiler was supplied via (hot) supply and (cold) return insulated piping at a temperature of 60 [°C] and a pressure of 2 bar. The radiative temperature for all internal elements was kept constant with the use of water-cooled wall elements.

For the measurement of the air temperature, two poles were placed across the middle section of the chamber. Each pole was equipped with four thermocouple sensors at the heights of 0.2 [m], 0.8 [m], 1.5 [m] and 2 [m], respectively. The accuracy of the thermocouples is ± 0.5 [°C] rated at tolerance class 1 providing accurate results. Concerning the mock target, three poles were placed across the middle section of the chamber, each one was equipped with one thermocouple sensor at 1 [m]. All mock targets were wrapped with a black tape of known emissivity [0.95]. The mock targets were equidistantly placed within the camber at 0.9 [m], 1.8 [m] and 2.7 [m], respectively from the left side wall, as seen in Fig. 2.

The indoor environmental chamber was imposed under transient conditions with varying air temperatures of approximately 20 [°C]–25 [°C]. Consecutive measurements with a time frame varying from 8 to 20 min were implemented. The time step was defined based on the rate of temperature increase, aiming to capture the temperature difference of 0,1 [°C]. The initial temperature of the environmental chamber was 20 [°C], and the measurements were resumed at a temperature of the environmental chamber of 25 [°C]. Statistical average values were provided for all three cases.

The data obtained from the sensors were retrieved by a data logger connected to a workstation. For the needs of the study, a FLIR E40BX thermal camera was employed. The IR resolution (array size) of this camera is 19,200 (160 × 120) pixels and the field of view is 25° × 19°V. Thermal camera specifications are provided in Table 1. For the post-processing of the results, FLIR Tools software [7] was used.

Table 1
Technical Specifications of Thermal Camera.

Technical Specification	Value
Field of view	25° × 19°V
IR Resolution (Array Size)	19,200 (160 × 120)
Thermal sensitivity	<0.045 °C (45 mK)
Frame Refresh	60 Hz
Temperature range	−20 °C to 120 °C (−4 to 248°F)
Accuracy	±2% rdg. or 2 °C

The experimental results were validated in two different ways: the measurements conducted with the use of thermocouples were used to verify the measurements delivered by the IR thermography. Also, the numerical model was validated with the use of experimental measurements. The model validation is described in Section 3.1.

2.2. Numerical simulation

A three-dimensional Finite Element Method (FEM) model was developed in COMSOL Multiphysics software [3], simulating the thermal chamber and the mock target poles. The analysis geometry consisted of four rectangular air layers and three cylindrical mock target poles. The width and depth of the air layers were 3.6 [m], respectively, representing the actual size of the experimental chamber (see Figs. 2–3). The height of the air layers starting from the bottom was 0.2 [m], 0.8 [m], 1.5 [m] and 2 [m], respectively. For this study, the element size preset for the mesh was set to extra fine with a total number of 985,141 elements, a minimum element quality of 0.06708 and an average

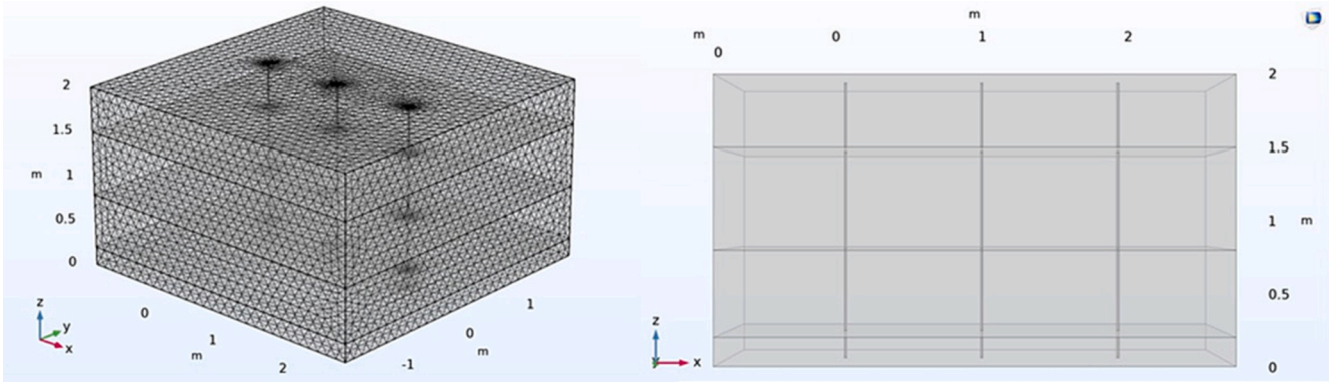

Fig. 3. Thermal Chamber – 3D Geometry – Mesh and Cross Section.

Table 2
Thermophysical properties materials used in numerical simulation.

Material	Density [kg/m^3]	Thermal Conductivity [W/m°C]	Heat Capacity [J/kg°C]
Air	1.23	0.025	1008
PVC (Mock Target)	1390	0.17	900

element quality of 0.6181. The mesh consisted of tetrahedra, triangle, edge and vertex elements. The total mesh volume was 25.92 [m^3] with an element volume ratio of 8.949^{-7} (Fig. 3).

The fundamental law governing the calculations with the FEM model was the conservation of energy equation [11]. For a fluid subjected to heat transfer, the resulting heat equation is:

$$\rho C_p\left(\frac{\partial T}{\partial t}+(\mathbf{u}\bullet\nabla)T\right)=-(\nabla\bullet\mathbf{q})+\tau:\mathbf{S}-\frac{T}{\rho}\frac{\partial\rho}{\partial T}\Big|_{\rho}\left(\frac{\partial\rho}{\partial t}+(\mathbf{u}\bullet\nabla)\rho\right)+Q \tag{1}$$

The heat transfer interfaces used Fourier's law of heat conduction, which states that the conductive heat flux, q, is proportional to the temperature gradient:

$$q_i=-k\frac{\partial T}{\partial x_i} \tag{2}$$

Also, the analysis assumed that mass is always conserved, which means that density and velocity are related through the equation.

$$\frac{\partial\rho}{\partial t}+\nabla\bullet(\rho\mathbf{v})=0 \tag{3}$$

The terms viscous heating (second term), pressure work (third term) and heat sources (fourth term) were ignored. To this end, the fundamental equation used was reordered as follows:

$$\rho C_p\frac{\partial T}{\partial t}+\rho C_p\mathbf{u}\bullet\nabla T=\nabla\bullet(k\nabla T) \tag{4}$$

Heat transfer in solids and fluids was assumed between the gaseous air (heat transfer in fluids) and the mock target poles (heat transfer in solids). The numerical analysis was conducted using the (GMRES) time dependant solver under transient conditions; with time steps ranges of (0,4,96), (0,4,120) and (0,4,240) minutes for air ventilation heating, underfloor heating, and radiator heating, respectively. The boundary conditions considered for the numerical analysis were the four air layers surrounding the mock target poles, where interpolated temperature profiles derived from the thermocouple measurements of the experimental phase were imposed on the corresponding height of each air layer for the three heating cases of air ventilation, underfloor heating and radiator heating. The thermophysical properties of the materials considered for the numerical analysis are presented in Table 2. The initial temperature of the model was set to 20 [°C]. In Fig. 14 the numerical model calculation is graphically demonstrated.

Table 3
Air Ventilation Heating – Temperature deviation [%] between measured room temperature and mock target surface temperature – All heights.

Temperature Deviation [%]				
Minutes	20 [cm]	80 [cm]	150 [cm]	200 [cm]
8	−1.65	−1.30	−2.06	−0.61
16	−2.16	−1.88	−2.57	−1.52
24	−2.87	−2.92	−3.84	−2.83
32	−3.97	−3.70	−4.13	−3.64
40	−3.53	−3.47	−3.59	−3.42
48	−2.27	−2.10	−2.67	−2.15
56	−3.22	−3.09	−3.48	−3.32
64	−3.09	−2.73	−3.04	−3.25
72	−3.17	−2.81	−3.34	−3.68
80	−2.70	−2.57	−2.87	−2.99
88	−2.23	−1.80	−2.20	−2.38
96	−1.82	−1.58	−1.77	−1.81

3. Results and discussions

3.1. Validation of mock target IR thermography and numerical simulation against measurements with thermocouples

The performance of the temperature measurements of the mock target IR thermography was validated against the measurements conducted with the use of thermocouples on the poles. Also, the temperature distribution on the poles provided by the numerical model was validated against the measurements delivered by the thermocouples on the poles.

Table 4
Radiator Heating – Temperature deviation [%] between measured room temperature and mock target surface temperature - All heights.

Temperature Deviation [%]				
Minutes	20 [cm]	80 [cm]	150 [cm]	200 [cm]
20	0.15	−0.27	−0.73	−1.10
40	1.10	0.66	−0.13	−0.26
60	0.40	−0.10	0.53	0.40
80	0.51	0.01	0.46	0.46
100	0.74	0.70	0.51	0.12
120	0.90	0.75	0.26	0.30
140	1.45	0.94	1.76	1.53
160	1.68	1.42	0.79	0.69
180	1.03	1.15	0.76	0.70
200	1.49	1.27	1.59	1.36
220	1.75	1.48	0.96	0.80
240	2.16	2.15	0.93	0.84

Table 5
Underfloor Heating – Temperature deviation [%] between measured room temperature and mock target surface temperature - All heights.

Temperature Deviation [%]				
Minutes	20 [cm]	80 [cm]	150 [cm]	200 [cm]
20	2.09	−1.22	−1.52	−0.62
40	5.63	−0.41	−0.30	0.84
60	6.83	0.47	−0.74	−0.08
80	7.96	1.45	0.39	1.06
100	7.98	1.18	0.41	0.98
120	8.24	1.03	0.72	1.69

Table 6
Air Ventilation Heating – Temperature deviation [%] between mock target surface temperature and simulated mock target surface temperature – All heights.

Temperature Deviation [%]				
Minutes	20 [cm]	80 [cm]	150 [cm]	200 [cm]
8	−0.81	−1.23	−0.95	−2.78
16	0.44	−0.30	0.61	−0.86
24	1.87	1.48	1.96	0.99
32	2.71	2.28	2.49	1.70
40	2.43	2.09	2.08	1.64
48	1.35	0.97	1.12	0.64
56	2.47	2.02	2.14	1.82
64	2.32	1.83	1.83	1.73
72	2.28	1.87	2.25	2.23
80	1.89	1.63	1.71	1.65
88	1.54	0.99	1.34	1.30
96	1.23	0.83	0.78	0.86

In Tables 3–5 the maximum temperature deviation between the measured temperature with the use of IR thermography and the measurements by employing thermocouples are presented. As can be deduced by the table values, the temperature deviation percentage for the cases of air ventilation, radiator and underfloor heating are −4.13 [%], 2.16 [%] and 8.24 [%] respectively. Similarly, the numerical model results were validated against the IR thermography measurements. The temperature deviation percentage data of the IR thermography mock target surface temperatures versus the simulated mock target surface temperatures are shown in Tables 6–8. Considering the ventilation, radiator and underfloor heating mechanisms, the maximum calculated errors were −2.78 [%], −5.31 [%] and −11.40 [%], respectively. It is observed that the temperature profile of both experimental and numerical data was identical with a low percentage of temperature deviation under all transient conditions. The numerical model approach proved to be effective, and the obtained results were in good agreement with the experimental results. Results of the numerical model are provided in Fig. 4 in time steps. The agreement between the numerical simulation and measurements is presented in Figs. 5–7 for all tested building technical heating systems.

3.2. Time response of mock target IR thermography

Considering the ventilation heating system, Figs. 8 and 9 graphically present the results of the IR thermography and measured air room data at the heights of 0.2 [m], 0.8 [cm], 1.5 [m] and 2 [m] with time intervals of 8 min. The highest temperatures were measured in the lower section of the thermal chamber since the ventilation system supplied the warm air downwards. From the bottom of the thermal chamber, the temperatures measured were observed to decrease as the level above the floor increased. Under transient conditions, it is observed that both temperature profiles of IR thermography and measured air room temperature cases followed an identical ascending order with good agreement. The time needed for the thermal chamber to reach 25 [°C] was 96 min, which was faster than both underfloor and radiator heating. Also, it was observed that the thermal performance of the mock target was sufficient, and the time needed to reach the room air temperature was approximately 16 min.

Table 7
Radiator Heating – Temperature deviation [%] between mock target surface temperature and simulated mock target surface temperature – All heights.

Temperature Deviation [%]				
Minutes	20 [cm]	80 [cm]	150 [cm]	200 [cm]
20	−1.53	−1.82	−3.63	−3.78
40	−1.95	−3.09	−4.15	−3.74
60	−0.99	−2.77	−5.31	−4.22
80	−2.14	−4.09	−4.56	−3.04
100	−1.95	−3.86	−4.64	−2.90
120	−2.30	−3.89	−4.25	−2.59
140	−2.44	−4.46	−4.77	−3.36
160	−2.20	−3.52	−4.73	−3.30
180	−2.34	−3.84	−3.49	−2.32
200	−2.90	−4.46	−4.49	−2.85
220	−2.87	−4.06	−3.79	−2.74
240	−2.63	−3.89	−3.80	−2.87

Table 8
Underfloor Heating – Temperature deviation [%] between mock target surface temperature and simulated mock target surface temperature – All heights.

Temperature Deviation [%]				
Minutes	20 [cm]	80 [cm]	150 [cm]	200 [cm]
20	−1.55	−1.56	−1.91	−1.25
40	−4.03	−2.00	−0.78	−1.69
60	−8.89	−5.31	−2.84	−4.32
80	−9.41	−5.81	−2.27	−4.06
100	−11.40	−7.68	−3.30	−5.23
120	−10.87	−6.98	−3.43	−5.49

For the investigation of radiator heating, the time needed for the thermal chamber to reach 25 [°C] was 240 min. The IR thermography measurements were performed every 20 min. Figs. 10 and 11 present the graphical data for the IR thermography and the air room temperature measurements. In contrast to ventilation heating, the air room temperature was increased as the level above the floor increased. The thermal chamber's airflow wasn't disrupted by any other mechanism, consequently, the hot air was rising due to its lower density and because of the heat that was introduced by the radiator. The IR thermography and the measured air room data were observed to be identical and indicated that the proposed technique was able to provide accurate measurements. The time needed for the mock target to reach the air room temperature was approximately 20 min, indicating sufficient thermal performance.

In the underfloor heating case, the time needed for the thermal chamber to reach 25 [°C] was 120 min. The IR thermography measurements were performed every 20 min. Figs. 12 and 13 present the graphical data for the IR thermography and the measured air room temperatures obtained. The air temperature distribution was observed to follow the same pattern as ventilation heating, the lowest temperatures were observed at the top of the thermal chamber and the temperature decreased as the level above the floor increased. Based on IR

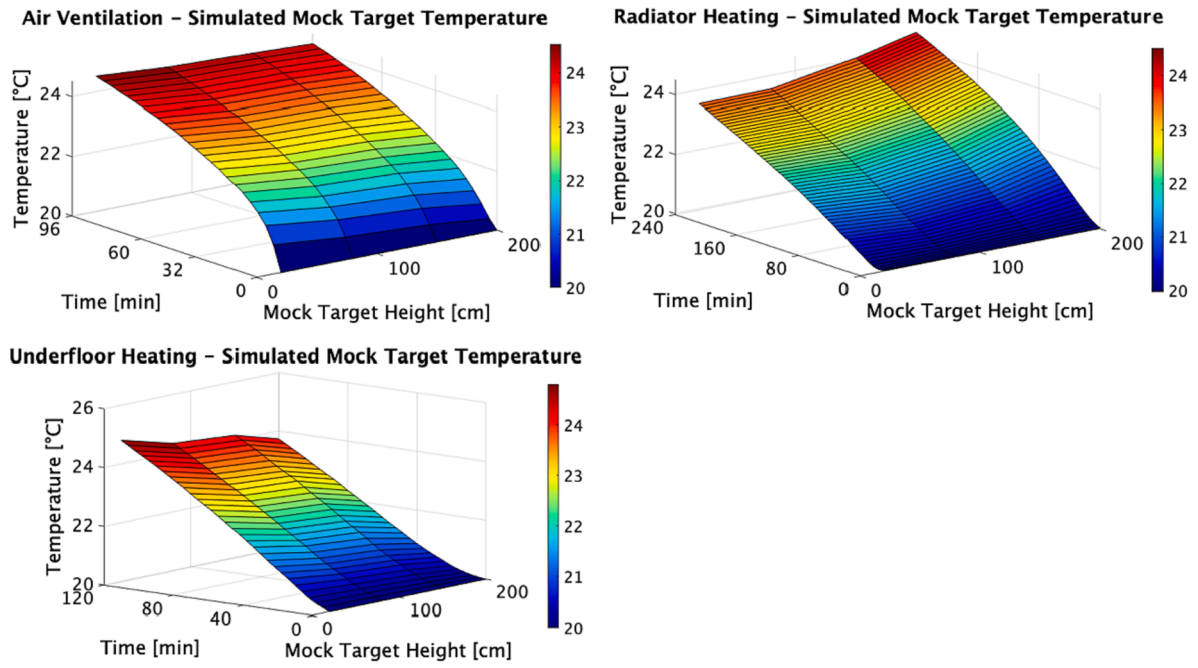

Fig. 4. FEM results – Simulated mock target temperature – Air ventilation, Radiator heating and Underfloor heating.

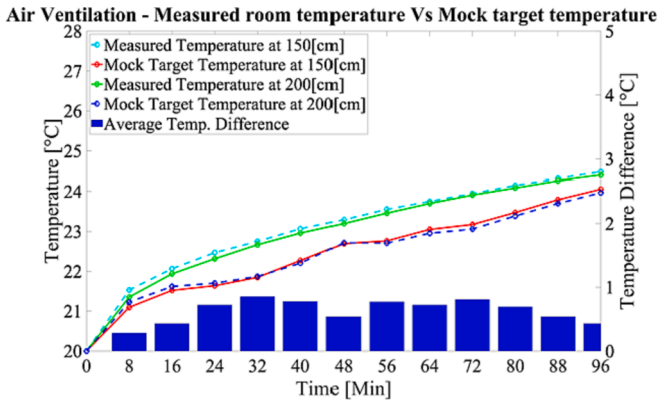

Fig. 5. Air Ventilation Heating – Measured room temperature Vs Mock target temperature – 150 [cm] and 200 [cm].

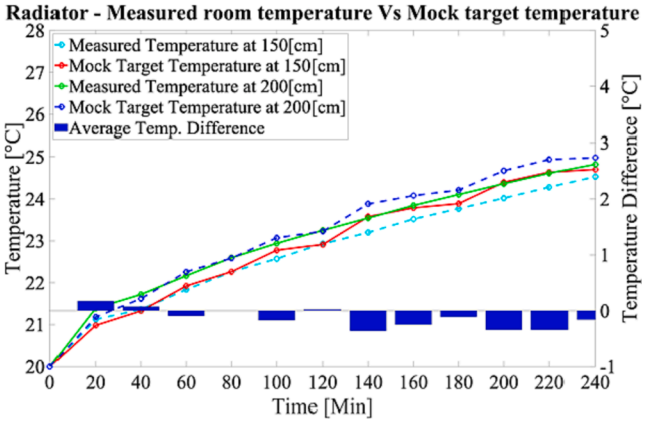

Fig. 6. Radiator Heating – Measured room temperature Vs Mock target temperature – 150 [cm] and 200 [cm].

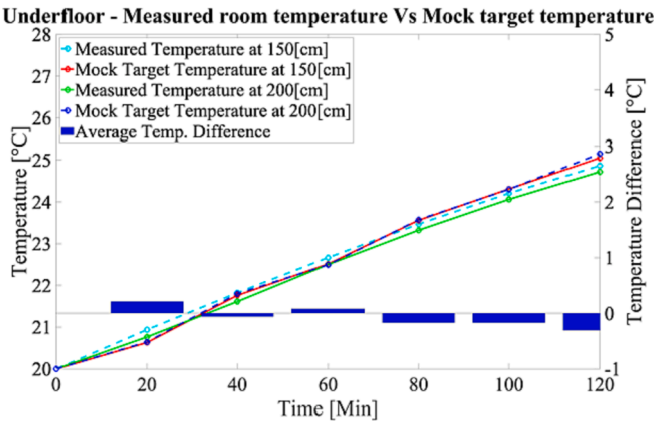

Fig. 7. Underfloor Heating – Measured room temperature Vs Mock target temperature – 150 [cm] and 200 [cm].

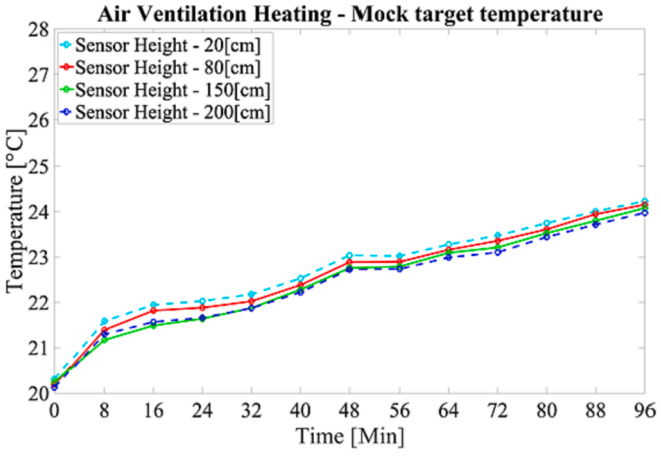

Fig. 8. Air Ventilation Heating – Mock target temperature.

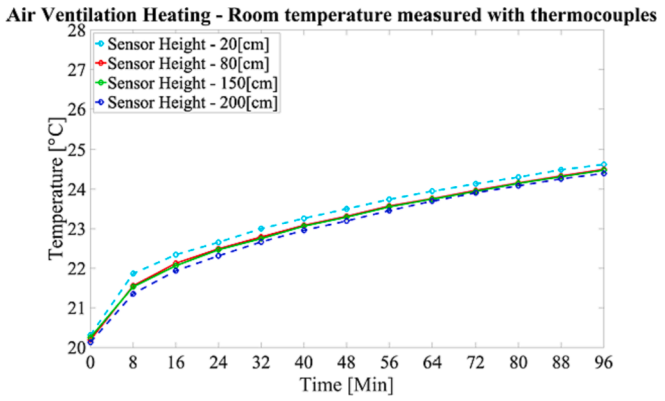

Fig. 9. Air Ventilation Heating – Room temperature measured with thermocouples.

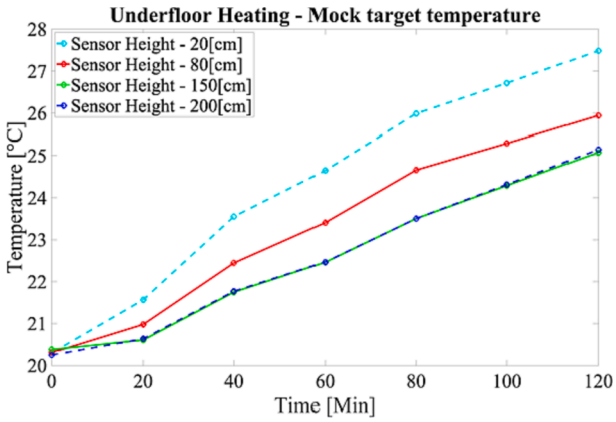

Fig. 12. Underfloor Heating – Mock target temperature.

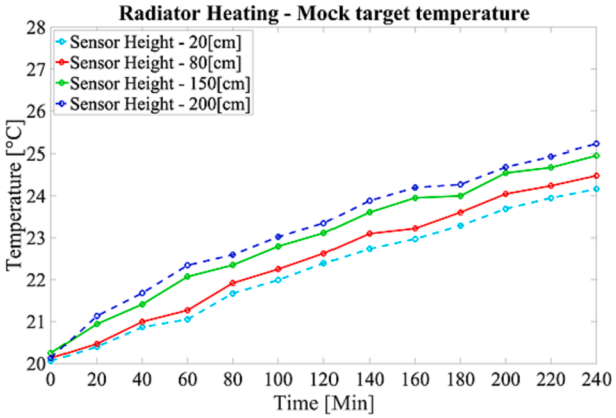

Fig. 10. Radiator Heating – Mock target temperature.

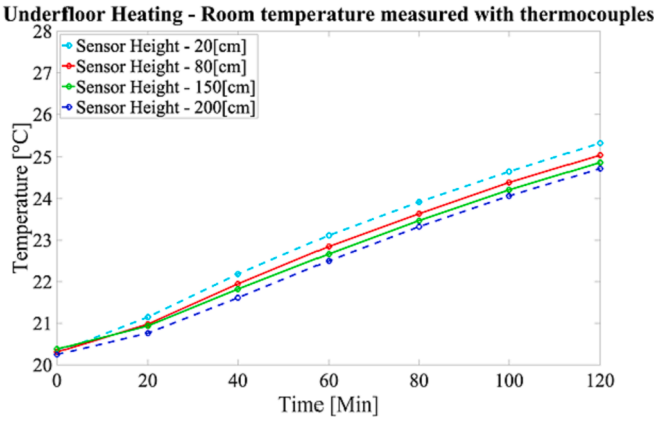

Fig. 13. Underfloor Heating – Room temperature measured with thermocouples.

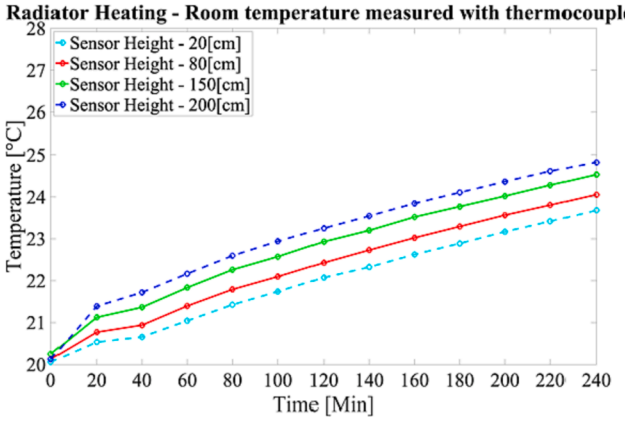

Fig. 11. Radiator Heating – Room temperature measured with thermocouples.

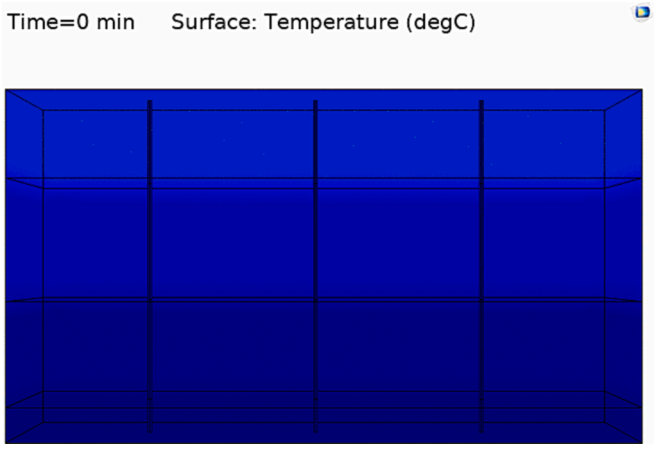

Fig. 14. Numerical Simulation – Radiator Heating – Surface Temperature – Time 0 to 240 min.

thermography data, the measurements were less accurate towards the bottom of the climate chamber. This was possibly caused by the heat released at a low level, which could have interfered with the measurement. The time lag between the thermal equilibrium of the air room and the mock target based on the measurements was approximately 20 min, revealing identical thermal performance to radiator heating.

4. Conclusions

The focus of this study was to evaluate the thermal performance of the mock target IR thermography technique under transient conditions. IR thermography measurements were employed to measure the mock target surface temperature under transient thermal conditions. To validate this approach a numerical model was developed using the computational tool COMSOL Multiphysics [3]. The IR thermography measurements and numerical model results were validated with the measurements provided by thermocouples. Considering the experimental conditions, the appropriate transient environment was achieved using three heating mechanisms of air ventilation, radiator and

underfloor heating in the environmental chamber of the Kaunas University of Technology. The results indicated that the mock target surfaces were thermally adapting at an adequate rate under transient conditions. It was observed that the temperature profile of the mock target surface was identical to the measured air room profile under the three heating methods, indicating that the IR thermography may provide accurate measurements, given that the appropriate time lag is considered. The time lag observed for the mock target methodology under thermally transient conditions was observed to be between 15 and 20 min, depending on the rate of change of temperature in space and the heating technique applied. It is hereby concluded that the mock target IR thermography may be adequately employed under transient conditions.

Funding details

The paper is a part of the dissemination activities of the research project "Development of Utilities Management Platform for the case of Quarantine and Lockdown" (Grant agreement ID: 101007641), funded by the European Commission.

CRediT authorship contribution statement

Loucas Georgiou: Conceptualization, Writing – original draft, Software. **.Laura Stasiuliene:** Data curation, Methodology. **Rokas Valancius:** Visualization, Investigation. **Lina Seduikyte:** Software, Validation. **Andrius Jurelionis:** Supervision. **Paris A. Fokaides:** Writing – review & editing.

Declaration of Competing Interest

The authors declare that they have no known competing financial interests or personal relationships that could have appeared to influence the work reported in this paper.

Data availability

Finite element model - https://github.com/LoucasGeo/Investigation-of-the-Performance-of-Mock-Target-IR-Thermography-for-Indoor-Air-Temperature-Measureme/releases/tag/v1.

Numerical Results - https://data.mendeley.com/datasets/3xs5c99wmh/1.

Appendix A. Supplementary material

Supplementary data to this article can be found online at https://doi.org/10.1016/j.measurement.2023.112461.

References

[1] I.F. Almesri, H.B. Awbi, Predictions of thermal comfort in stratified room environment, in: Building Simulation, Vol. 4, No. 2, Tsinghua Press, 2011, pp. 169–180.
[2] L. Catalina, A. Doru, C. Calin, The use of thermographic techniques and analysis of thermal images to monitor the respiratory rate of premature new-borns, Case Stud. Therm. Eng. 25 (2021), 100926, https://doi.org/10.1016/J.CSITE.2021.100926.
[3] COMSOL Multiphysics, n.d., URL https://www.comsol.com/comsol-multiphysics.
[4] B. Dai, Y. Tong, Q. Hu, Z. Chen, Characteristics of thermal stratification and its effects on HVAC energy consumption for an atrium building in south China, Energy 249 (2022), 123425.
[5] R.G. Dourado da Silva, D.C. Ferreira, F.V. Avelar Dutra, S.M.M. Lima e Silva, Simultaneous real time estimation of heat flux and hot spot temperature in machining process using an infrared camera, Case Stud. Therm. Eng. 28 (2021), 101352, https://doi.org/10.1016/J.CSITE.2021.101352.
[6] F.B. Errebai, L. Derradji, M. Amara, Thermal behaviour of a dwelling heated by different heating systems, Energy Proc. 107 (2017) 144–149.
[7] FLIR, FLIR Tools Software for PC and Mac, 2015.
[8] P.A. Fokaides, R. Apanaviciene, J. Černeckiene, A. Jurelionis, E. Klumbyte, V. Kriauciunaite-Neklejonoviene, D. Pupeikis, D. Rekus, J. Sadauskiene, L. Seduikyte, L. Stasiuliene, J. Vaiciunas, R. Valancius, T. Ždankus, Research challenges and advancements in the field of sustainable energy technologies in the built environment, Sustainability 12 (2020) 8417, https://doi.org/10.3390/su12208417.
[9] P.A. Fokaides, A. Jurelionis, L. Gagyte, S.A. Kalogirou, Mock target IR thermography for indoor air temperature measurement, Appl. Energy 164 (2016), https://doi.org/10.1016/j.apenergy.2015.12.025.
[10] P.A. Fokaides, S.A. Kalogirou, Application of infrared thermography for the determination of the overall heat transfer coefficient (U-Value) in building envelopes, Appl. Energy 88 (2011), https://doi.org/10.1016/j.apenergy.2011.05.014.
[11] S. Whitaker, Fundamental Principles of Heat Transfer, Elsevier, 2013.
[12] O.B. Kazanci, M. Shukuya, A theoretical study of the effects of different heating loads on the exergy performance of water-based and air-based space heating systems in buildings, Energy 238 (2022), 122009.
[13] A. Kylili, P.A. Fokaides, P. Christou, S.A. Kalogirou, Infrared thermography (IRT) applications for building diagnostics: a review, Appl. Energy 134 (2014), https://doi.org/10.1016/j.apenergy.2014.08.005.
[14] R. Lapisa, M.O. Abadie, E. Bozonnet, P. Salagnac, Numerical Analysis of the Thermal Stratification Modelling Efect on Comfort for the Case of a Commercial Low-Rise Building, 2014.
[15] M. Maivel, A. Ferrantelli, J. Kurnitski, Experimental determination of radiator, underfloor and air heating emission losses due to stratification and operative temperature variations, Energy Build. 166 (2018) 220–228.
[16] A. Prozuments, A. Borodinecs, Indoor air stratification in warm air supply systems, ASHRAE J. 59 (11) (2017) 54–64.
[17] B. Ramzan, M.S. Malik, M. Martarelli, H.T. Ali, M. Yusuf, S.M. Ahmad, Pixel frequency based railroad surface flaw detection using active infrared thermography for Structural Health Monitoring, Case Stud. Therm. Eng. 27 (2021), 101234, https://doi.org/10.1016/J.CSITE.2021.101234.
[18] L. Seduikyte, L. Stasiulienė, T. Prasauskas, D. Martuzevičius, J. Černeckienė, T. Ždankus, M. Dobravalskis, P. Fokaides, Field measurements and numerical simulation for the definition of the thermal stratification and ventilation performance in a mechanically ventilated sports hall, Energies 12 (2019) 2243, https://doi.org/10.3390/en12122243.
[19] P. Seiwert, L. Schmitt, M. Wesseling, D. Müller, Detection of vertical air temperature distribution by long-wave infrared thermography, Roomvent & Ventilation 2018 (2018) 403–408.
[20] Z. Wang, M. Luo, Y. Geng, B. Lin, Y. Zhu, A model to compare convective and radiant heating systems for intermittent space heating, Appl. Energy 215 (2018) 211–226.
[21] S. Wiriyasart, P. Naphon, Numerical study on air ventilation in the workshop room with multiple heat sources, Case Stud. Therm. Eng. 13 (2019), 100405, https://doi.org/10.1016/J.CSITE.2019.100405.
[22] J. Yang, Z. Dong, H. Yang, Y. Liu, Y. Wang, F. Chen, H. Chen, Numerical and experimental study on thermal comfort of human body by split-fiber air conditioner, Energies 15 (10) (2022) 3755.